Optical Stark spectroscopy of molecular aggregates

Shaul Mukamel, Pavel Rott,[a] and Vladimir Chernyak
Department of Chemistry, University of Rochester, Rochester, New York 14627

(Received 21 August 1995; accepted 4 January 1996)

Effects of static disorder and interaction with phonons on the dynamics of Frenkel excitons in molecular aggregates are studied by calculating the absorption of a weak probe in the presence of a strong resonant and off-resonant pump field. To second order in the pump amplitude, the self-energy which determines the Stark shift and dynamical broadening of the probe absorption is expressed in terms of the single exciton Green function and the two-exciton scattering matrix. For stronger pump intensities the self-energy is calculated using higher-order optical response functions of the system. © *1996 American Institute of Physics.* [S0021-9606(96)01314-4]

I. INTRODUCTION

The nature of electronic excitations of molecular aggregates is a fundamental problem with important practical implications.[1–4] Studies of size dependence of optical response provide a unique insight into the connection between properties of individual molecules and bulk properties of materials.[5] The structure and dynamics of molecules is commonly interpreted using their electronic and vibrational eigenstates. Molecular[6,7] and semiconductor[8,9] crystals are on the other hand best described using collective (quasiparticle) excitations such as excitons and phonons. Small aggregates may be treated using both pictures, thus clarifying the connection between them. From the practical side, strongly coupled aggregates of dye molecules (e.g., cyanide dyes) known as *J* aggregates play an important role in photosensitization of semiconductor particles which is the primary step in photography.[3,9–13] Organic nanostructures such as monolayers and multiple quantum wells show interesting photoinduced charge transfer properties which can be used in electroluminescence devices and nonlinear optical switches.[14] Molecular aggregates have numerous important biological functions. These include the conversion of light energy into chemical energy by collecting the light and channelling it into the necessary sites by the light harvesting antenna systems, and the intermolecular charge transfer in the photosynthetic reaction center.[15–18]

The electronic structure of molecular aggregates may be described using the Frenkel-exciton Hamiltonian.[6] The linear optical response is determined by the properties of one-exciton states, whereas multiexciton states can be probed using a variety of nonlinear spectroscopic techniques in the frequency and time domain.[5,19] Multiexciton states are crucial in determining how nonlinear susceptibilities scale with aggregate size.[5]

In this paper we calculate the pump–probe frequency-domain spectrum of molecular aggregates using the Frenkel exciton model, including static disorder and exciton–phonon coupling. For off-resonant pump (i.e., when the pump frequency is tuned outside the exciton band), the probe absorption shifts with the pump intensity. This ''optical Stark shift'' is analogous to the ordinary Stark effect induced by a static (dc) electric field.[20] Pump–probe spectroscopy monitors the linear absorption of a weak probe in the presence of a strong pump field. Since the system is excited by the pump, multiexciton states become accessible. For sufficiently weak pump and probe this spectroscopy can be described as a four-wave mixing process. The signal is then expressed in terms of the linear and third-order nonlinear response functions $R^{(1)}$ and $R^{(3)}$, and involves one- and two-exciton states only.[19] The one-exciton to two-exciton transition has been observed in disordered *J* aggregates.[21] For higher pump fields the optical Stark effect has been observed in anisotropic molecular crystals,[22] *J* aggregates,[23] direct-gap semiconductors,[24] polydiacetylene and conjugated polymers.[25–27] The theoretical interpretation of the dynamical Stark effect beyond the two-level model (which is inapplicable for small detuning) was developed by Schmitt-Rink, Chemla, and Haug.[28] Combescot and Combescot[29] highlighted the important role of two-exciton states for near-resonance excitation and discussed the effect of Coulomb interaction between $e-h$ pairs for different detuning regimes. Later, Zimmermann,[30] has discussed the interband and intraband Stark effect for quantum wells to second order in the pump amplitude. Another interesting aspect of the dynamical Stark effect, namely, the ultrafast (femtosecond) response time reflecting exciton dynamics in quantum-well structures[24,31] is useful for optical gating and generation of ultrashort electrical pulses.[32] The Stark shift of *J* aggregates in strong pump fields involving multiexciton states has been investigated both experimentally[33] and theoretically.[34] Electroabsorption measurements[35] have shown both dynamical broadening and Stark shift. The present theory applies for off-resonant as well as resonant pump frequencies. When the pump is tuned inside the exciton band the picture becomes more complicated since real excitations are created and both coherent motion of two-exciton states and exciton transport affect the spectrum. We show how the Stark shift and dynamical broadening induced by an intense pump provide clear signatures for disorder and phonon effects in the exciton motion. We will demonstrate how the interplay of two-exciton coherent motion and exciton transport manifests itself in the Stark effect. This makes optical Stark

[a]Also at: Department of Physics and Astronomy, University of Rochester, Rochester, NY 14627.

spectroscopy a useful tool for studying exciton properties in molecular aggregates.

In Sec. II we present the model Hamiltonian of a molecular aggregate with electronic and nuclear degrees of freedom. The induced polarization to first order in the probe is expressed in terms of correlation functions of the polarization operators. In order to calculate the probe absorption we need to expand the optical polarization to first order in the probe, but retain high-order contributions in the pump. This is accomplished by introducing the pump-induced Stark self-energy $\Sigma^{(s)}$ whose real part determines the shift while the imaginary part results in dynamical broadening. The Stark self-energy can be expanded in powers of the pump field and the expansion coefficients expressed in terms of the optical response functions. We derive Green function expressions for the Stark self-energy to first order in the pump intensity. The self-energy is expressed in terms of the one-exciton Green function and two-exciton scattering matrix. The expressions for the Green function and scattering matrix are given in the site representation and apply to an arbitrary aggregate geometry. A recently developed Green function theory of four wave mixing spectroscopy of confined excitons including exciton–exciton interaction, phonons, and static disorder[4,7] will be used in calculations presented in the coming sections. In Sec. III we specialize to periodic aggregates and provide closed expressions for the necessary Green functions in **k** space. Numerical calculations for a one-dimensional aggregate with no additional degrees of freedom (other than electronic) are presented. In Sec. IV we repeat the numerical calculations of Sec. III for an aggregate with static diagonal disorder. Exciton–phonon interaction is incorporated in Sec. V. Our results are summarized in Sec. VI where we also connect the Stark self-energy with higher-order nonlinear response functions.

II. REAL SPACE GREEN FUNCTION EXPRESSION FOR THE PROBE ABSORPTION

The dynamics of electronic excitations in molecular aggregates can be modeled using the Frenkel exciton Hamiltonian which represents an assembly of interacting two-level molecules:[6]

$$\hat{H}_{\rm mat}(\xi)=\sum_n \Omega_n(\xi)\hat{B}_n^+\hat{B}_n+\sum_{m\neq n} J_{mn}(\xi)\hat{B}_m^+\hat{B}_n+\hat{H}'(\xi). \tag{2.1}$$

Here $\hat{B}_m(\hat{B}_m^+)$ is the exciton annihilation (creation) operator for the mth molecule that satisfy the Pauli commutation relations

$$[\hat{B}_m,\hat{B}_n^+]=(1-2\hat{B}_n^+\hat{B}_n)\delta_{mn}, \tag{2.2}$$

Ω_m is the electronic excitation energy of the mth molecule and J_{nm} is the intermolecular coupling responsible for exciton hopping. ξ stands for additional degrees of freedom (e.g., molecular vibrations, phonons, solvent, etc.) described by the Hamiltonian $\hat{H}'$. Their coupling with the excitons enters through the ξ dependence of $\Omega_n(\xi)$ and $J_{mn}(\xi)$. We have used the Heitler–London approximation for the intermolecular coupling which conserves the number of excitons and can only induce exciton hopping. This is justified in molecular aggregates where typically $|J_{nm}|\ll\Omega_n$. Consequently the ground state is the vacuum state with no excitons, and the purely electronic problem (with no additional degrees of freedom) is exactly solvable. The additional degrees of freedom make this a genuine many-body problem which may only be solved approximately. The coupling with radiation field $\mathscr{E}(\mathbf{r},t)$ is given by

$$\hat{H}_{\rm int}(t)=-\int d\mathbf{r}\ \mathscr{E}(\mathbf{r},t)\cdot\hat{P}(\mathbf{r}). \tag{2.3}$$

Here the polarization operator $\hat{P}(\mathbf{r})$ has the form:[36,37]

$$\begin{aligned}&\hat{P}(\mathbf{r})=\Sigma\hat{P}_m(\mathbf{r}),\\ &\hat{P}_m(\mathbf{r})=|\mu|\rho(\mathbf{r}-\mathbf{R}_m)(\hat{B}_m+\hat{B}_m^+),\end{aligned} \tag{2.4}$$

where $\rho(\mathbf{r}-\mathbf{R_m})$ is the normalized polarization density and μ is the transition dipole.

The following calculations use a compact correlation function expression for the optical response functions,[4] which are based on nonequilibrium Green function formalism, first introduced by Keldysh.[38] For an arbitrary operator $\hat{Q}$ we define the Heisenberg operator $\hat{Q}(t)$ whose evolution is determined by the material Hamiltonian $\hat{H}_{\rm mat}$ (i.e., without the external field). For any set of operators $\hat{Q}^{(1)}_{,\ldots,}\hat{Q}^{(n)}$ we introduce the following correlation function

$$\langle\hat{Q}^{(1)}_{\alpha_1}(t_1)\cdots\hat{Q}^{(n)}_{\alpha_n}(t_n)\rangle\equiv{\rm Tr}\{\hat{\rho}\hat{T}_{\alpha_1\ldots\alpha_n}[\hat{Q}^{(1)}(t_1)\ldots\hat{Q}^{(n)}(t_n)]\}, \tag{2.5}$$

where $\hat{\rho}$ is the equilibrium density matrix of the system, and the indices $\alpha_1\ldots\alpha_n$ assume the values L (left) and R (right). Equation (2.5) should be understood as follows: All operators with $L(R)$ should be placed to the left (right) of the density matrix. Furthermore, $\hat{T}_{\alpha_1\ldots\alpha_n}$ denotes a time-ordering operator which acts in the following manner: all L operators are ordered antichronologically (earlier times last) whereas the reverse (chronological) ordering is applied to the R operators. Using this notation, the order of operators in the lhs of Eq. (2.5) is immaterial since we have a unique prescription for ordering them based on their labels and time arguments. We next introduce the following combinations of left and right operators.

$$\begin{aligned}&Q_-\equiv Q_L-Q_R,\\ &Q_+\equiv\tfrac{1}{2}(Q_L+Q_R).\end{aligned} \tag{2.6}$$

The expectation value of the polarization $P(\mathbf{r},t)$ in the driven system is[4]

$$P(\mathbf{r},t)=\left\langle\hat{P}_+(\mathbf{r},t)\exp\left[i\int d\mathbf{r}'\int_{-\infty}^{+\infty}dt'\ \mathscr{E}(\mathbf{r}',t')\hat{P}_-(\mathbf{r}',t')\right]\right\rangle. \tag{2.7}$$

In a frequency-domain pump–probe measurement, the electric field is given by

$$\mathscr{E}(\mathbf{r},t)=\mathscr{E}_p e^{i\mathbf{k}_p\mathbf{r}-i\omega_p t}+\mathscr{E}_s e^{i\mathbf{k}_s\mathbf{r}-i\omega_s t}+{\rm c.c.}, \tag{2.8}$$

where $\mathscr{E}_p$ represents a strong pump field whereas $\mathscr{E}_s$ is a weak probe. Expanding the polarization to first order in the probe, we have

$$P(\mathbf{r},t)=\int d\mathbf{r}'\ dt'\ \mathscr{R}(\mathbf{r},t,\mathbf{r}',t;[\mathscr{E}_p])\mathscr{E}_s(\mathbf{r}',t'), \tag{2.9}$$

where $\mathscr{R}$ denotes the linear response function of the system driven by the pump alone. The formal expression of the response function can be obtained by perturbative expansion of Eq. (2.7) which yields

$$\mathscr{R}(\mathbf{r},t,\mathbf{r}',t';[\mathscr{E}_p])$$
$$=i\left\langle \hat{P}_+(\mathbf{r},t)\hat{P}_-(\mathbf{r}',t)\exp\left[i\int d\mathbf{r}''\ dt''\right.\right.$$
$$\left.\left.\times\mathscr{E}_p(\mathbf{r}'',t'')\hat{P}_-(\mathbf{r}'',t'')\right]\right\rangle. \tag{2.10}$$

We next expand the response function in powers of the pump, resulting in

$$\mathscr{R}(\mathbf{r},t;\mathbf{r}',t';[\mathscr{E}_p])$$
$$=i\langle\hat{P}_+(\mathbf{r},t)\hat{P}_-(\mathbf{r}',t')\rangle$$
$$+i^2\int d\mathbf{r}''\ dt''\langle\hat{P}_+(\mathbf{r},t)\hat{P}_-(\mathbf{r}',t')\hat{P}_-(\mathbf{r}'',t'')\rangle$$
$$\times\mathscr{E}_p(\mathbf{r}'',t'')+\cdots. \tag{2.11}$$

Successive terms in this expansion require the evaluation of higher-order correlation functions of the dipole operator. For a weak pump it is sufficient to truncate the sum to second order in $\mathscr{E}_p$. The necessary correlation function $\langle P_+P_-P_-P_-\rangle$ then represents the third-order response. For a strong pump we need to sum the series to infinite order. This can be done approximately using diagrammatic techniques.[4] To present the result we define the bare one-exciton Green function $G_{mn}(\omega)$:

$$G_{mn}(\omega)=-i\int_0^\infty dt\ e^{i\omega t}\langle\hat{B}_n(t)\hat{B}_m^+(0)\rangle. \tag{2.12}$$

We further introduce the two-exciton Green function $G^{(2)}$:[37]

$$G^{(2)}_{nm_1m_2m_3}(-\omega_s;\omega_1,-\omega_2,\omega_3)$$
$$\equiv\int_0^\infty\int_0^\infty\int_0^\infty dt_1\ dt_2\ dt_3\ e^{-i(\omega_1t_1-\omega_2t_2+\omega_3t_3)}$$
$$\times\langle\hat{B}_{n+}(0)\hat{B}_{m_2-}(t_2)\hat{B}^+_{m_1-}(t_1)\hat{B}^+_{m_3-}(t_3)\rangle, \tag{2.13}$$

which satisfies the Bethe–Salpeter equation

$$G^{(2)}_{nm_1m_2m_3}(-\omega_2;\omega_1,-\omega_2,\omega_3)$$
$$=\sum_{n'm_1'm_2'm_3'}G_{nn'}(\omega_s)G_{m_2'm_2}(\omega_2)$$
$$\times\overline{\Gamma}^{(t)}_{n'm_1'm_2'm_3'}(-\omega_s;\omega_1,-\omega_2,\omega_3)G_{m_2'm_1}(\omega_1)$$
$$\times G_{m_3'm_3}(\omega_3), \tag{2.14}$$

where $\overline{\Gamma^{(t)}}$ is the two-exciton scattering matrix.[38,39]

Using these quantities, we obtain the following expression for the response to first order in $\mathscr{E}_s$, and partially resumed to infinite order in $\mathscr{E}_p$

$$\mathscr{R}(\mathbf{r},t,\mathbf{r}',t';[\mathscr{E}_p])=\sum_{mn}\rho(\mathbf{r}-\mathbf{R}_m)\rho(\mathbf{r}'-\mathbf{R}_n)$$
$$\times\int\frac{d\omega}{2\pi}\mathscr{R}_{mn}(\omega,[\mathscr{E}_p])e^{-i\omega(t-t')}, \tag{2.15}$$

with

$$\mathscr{R}_{mn}(\omega,[\mathscr{E}_p])=\mu^2\{\mathscr{G}_{mn}(\omega,[\mathscr{E}_p])+\mathscr{G}^*_{nm}(\omega,[\mathscr{E}_p])\}. \tag{2.16}$$

The one exciton Green function $\mathscr{G}_{mn}(\omega,[\mathscr{E}_p])$ for the system driven by the pump field is defined as follows. We first introduce the time-domain Green function $\mathscr{G}_{mn}(t,t';[\mathscr{E}_p])$ in the presence of the pump field:

$$\mathscr{G}_{mn}(t,t',[\mathscr{E}_p])\equiv-i\left\langle\hat{B}_{m-}(t)\hat{B}_{n+}(t')\right.$$
$$\left.\times\exp\left[i\int d\tau\ d\mathbf{r}\ \hat{P}_-(\mathbf{r},\tau)\mathscr{E}_p(\mathbf{r},\tau)\right]\right\rangle. \tag{2.17}$$

Since the pump field is monochromatic [Eq. (2.8)], this Green function can be expanded as

$$\mathscr{G}_{mn}(t,t',[\mathscr{E}_p])$$
$$=\sum_{N=-\infty}^{+\infty}\int\frac{d\omega\ d\omega'}{(2\pi)^2}e^{-i\omega t+i\omega' t'}$$
$$\times2\pi\delta(\omega-\omega'-2\omega_pN)\mathscr{G}^{(N)}_{mn}(\omega;[\mathscr{E}_p]). \tag{2.18}$$

The Green function in Eq. (2.16) is defined as $\mathscr{G}_{mn}(\omega,[\mathscr{E}_p])\equiv\mathscr{G}^{(0)}_{mn}(\omega,[\mathscr{E}_p])$. It can be obtained by solving the Dyson equation

$$\mathscr{G}_{mn}(\omega,[\mathscr{E}_p])=G_{mn}(\omega)+\sum_{m'n'}G_{mm'}(\omega)$$
$$\times\Sigma^{(s)}_{m',n'}(\omega,[\mathscr{E}_p])\mathscr{G}_{n'n}(\omega,[\mathscr{E}_p]). \tag{2.19}$$

Equations (2.16) and (2.19) were obtained using the diagrammatic technique introduced in Ref. 4, where a single line stands for the exciton Green function $\mathscr{G}$ and $\overline{\Gamma^{(t)}}$ denotes the two-exciton scattering matrix. $\mathscr{R}(\omega,[\mathscr{E}_p])$ can be ex-

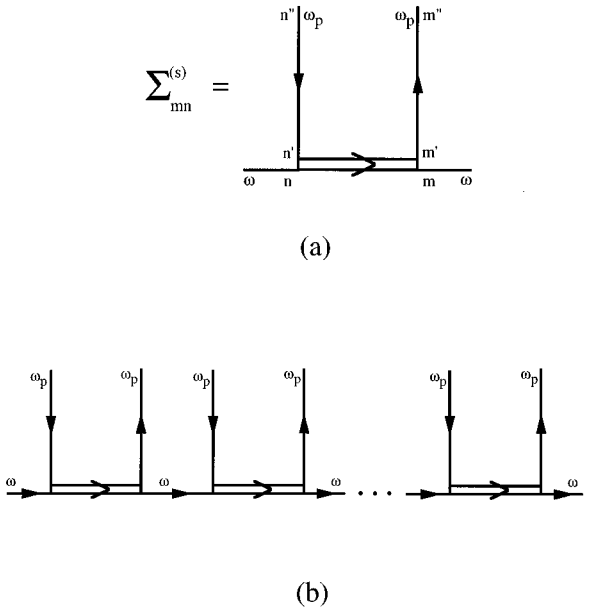

FIG. 1. Diagrams contributing to the Stark signal. (a) Stark self-energy $\Sigma^{(s)}$ to the second order in the pump field [Eq. (2.20)]. (b) Diagrams contributing to the polarization [Eqs. (2.16) and (2.19)].

pressed as a sum of diagrams with two external lines carrying the probe frequency ω and arbitrary number of external lines carrying the pump frequency ω_p. The latter determines the order with respect to the pump field. When ω is in the absorption region, to avoid the compensation of the small factors related to the pump field by large resonant factors $G(\omega)$ we introduce the sum of diagrams contributing to $\mathscr{R}$ which do not contain these resonant factors and denote this sum by $\Sigma^{(s)}(\omega,[\mathscr{E}_p])$. This leads to the Dyson equation (2.19). Since the real and imaginary parts of $\Sigma^{(s)}(\omega,[\mathscr{E}_p])$ determine the shift and the broadening respectively of the absorption line induced by the pump, we will refer to $\Sigma^{(s)}_{nm}(\omega,[\mathscr{E}_p])$ as the Stark self-energy. It can be expanded in even powers of the pump field $\mathscr{E}_p$, and the leading (second order) term is given by diagrams with two external lines carrying the pump frequency ω_p as shown in Fig. 1(a). Note that the polarization which is related to $\mathscr{G}_{mn}$ is given in this approximation by the infinite sum of diagrams shown in Fig. 1(b) containing all orders of the pump field. [This means that if the Green function $\mathscr{G}$ is given by diagrams presented in Fig. 1(b), it can be expressed in the form of Eq. (2.19), with $\Sigma^{(s)}$ presented diagrammatically in Fig. 1(a) and given by Eq. (2.20).] The Stark self-energy can therefore be expressed in terms of the bare Green function and the two-exciton scattering matrix:

$$\Sigma^{(s)}_{nm}(\omega,[\mathscr{E}_p])=\mu^2\sum_{m'n'm''n''}\overline{\Gamma}^{(t)}_{nm'n'm}(-\omega;\omega_p,-\omega_p,\omega)\times G_{m'm''}(\omega_p)G^{*}_{n'n''}(\omega_p)\mathscr{E}_{m''}\mathscr{E}^{*}_{n''}. \tag{2.20}$$

Equation (2.16) together with (2.12), (2.19), and (2.20) constitutes the main formal result of the present article which will be used in the coming sections.

III. PUMP–PROBE SPECTROSCOPY OF PERIODIC AGGREGATES

In periodic aggregates the exciton Green function introduced in Sec. II can be further simplified by switching to momentum $\mathbf{k}$ space, we adopt the following convention: $d\mathbf{k}=(2\pi/a)^d\,d^dk$, where a is the lattice constant and d is the dimension of an aggregate. Molecular monolayers and multilayers have a two-dimensional periodicity. In this section we consider a perfect one-dimensional aggregate with nearest neighbor interactions and neglect the additional ξ degrees of freedom. This model can serve as an excellent starting point for the simulation of optical properties of J aggregates. The optical response of cyclic periodic aggregates have been considered in Ref. 12. The photosynthetic antenna complexes have a circular geometry with 9, 12, and 18 chromophores.[15]

The one exciton Green function $G(\omega,\mathbf{k})$ is now given by

$$G(\omega,\mathbf{k})=\frac{1}{\omega-\epsilon(\mathbf{k})+i\,\eta(\mathbf{k})/2}, \tag{3.1}$$

where $\epsilon(\mathbf{k})$ is a dispersion relation for free excitons, and $\eta(\mathbf{k})$ is a phenomenological momentum-dependent scattering matrix. The two-exciton scattering matrix has the following form in the momentum domain:

$$\overline{\Gamma}^{(t)}(-\omega_s-\mathbf{k}_s;\omega_1\mathbf{k}_1,-\omega_2-\mathbf{k}_2,\omega_3\mathbf{k})=\overline{\Gamma}^{(a)}(-\omega_s-\mathbf{k}_s;\omega_1\mathbf{k}_1,-\omega_2-\mathbf{k}_2,\omega_3\mathbf{k}_3), \tag{3.2}$$

$$\overline{\Gamma}^{(a)}(-\omega_s-\mathbf{k}_s;\omega_1\mathbf{k}_1,-\omega_2-\mathbf{k}_2,\omega_3\mathbf{k}_3)\equiv\overline{\Gamma}(\omega_1+\omega_3,\mathbf{k}_1+\mathbf{k}_3), \tag{3.3}$$

with

$$\overline{\Gamma}(\omega,\mathbf{k})\equiv-2\left\{\int\frac{d\omega'\,d\mathbf{p}}{2\pi i}\,G(\omega',\mathbf{p})G(\omega-\omega',\mathbf{k}-\mathbf{p})\right\}^{-1}. \tag{3.4}$$

[The momentum dependence of $\overline{\Gamma}^{(a)}$ given by Eq. (3.3) follows from the following real space relation: $\Gamma^{(a)}_{nm_1m_2m_3}=\delta_{nm_2}\delta_{m_1m_3}\overline{\Gamma}_{nm_1}$.]

The Stark self-energy is given by

$$\Sigma^{(s)}(\omega,\mathbf{k};\omega_p,\mathbf{k}_p,[\mathscr{E}_p])=\mu^2\overline{\Gamma}^{(t)}(-\omega-\mathbf{k};\omega_p\mathbf{k}_p,-\omega_p-\mathbf{k}_p,\omega\mathbf{k})|G(\omega_p,\mathbf{k}_p)|^2|\mathscr{E}|^2. \tag{3.5}$$

The response function now becomes

$$\mathscr{R}(\omega\mathbf{k};\omega_p\mathbf{k}_p,[\mathscr{E}_p])=\mu^2[\mathscr{G}(\omega\mathbf{k};\omega_p\mathbf{k}_p,[\mathscr{E}_p])+\mathscr{G}^{*}(-\omega-\mathbf{k};\omega_p\mathbf{k}_p,[\mathscr{E}_p])], \tag{3.6}$$

with

$$\mathscr{G}(\omega\mathbf{k};\omega_p\mathbf{k}_p,[\mathscr{E}_p])=\{\omega-\epsilon(\mathbf{k})+i\,\eta(\mathbf{k})/2-\Sigma^{(s)}(\omega\mathbf{k};\omega_p\mathbf{k}_p,[\mathscr{E}_p])\}^{-1}. \tag{3.7}$$

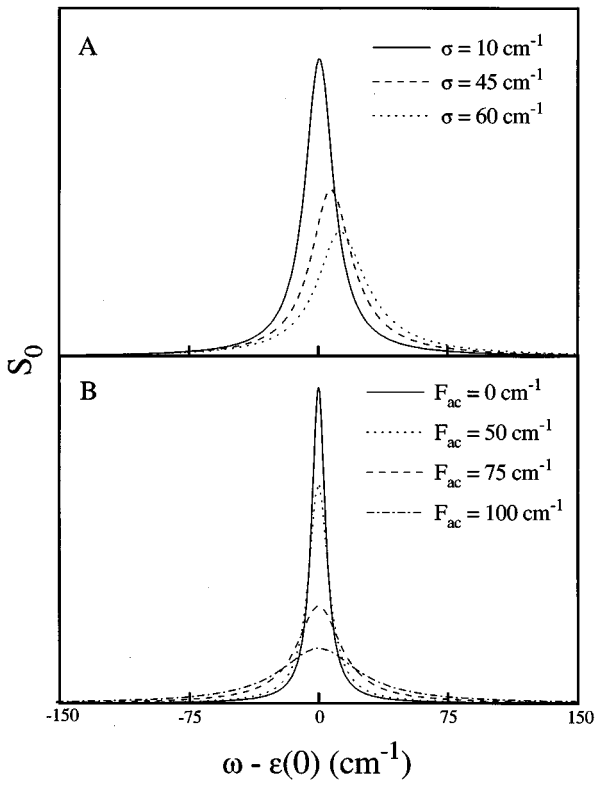

FIG. 2. Linear absorption for a periodic one-dimensional aggregates. (a) System with various diagonal disorder parameter, (b) system with various exciton-phonon coupling; for other parameters see text.

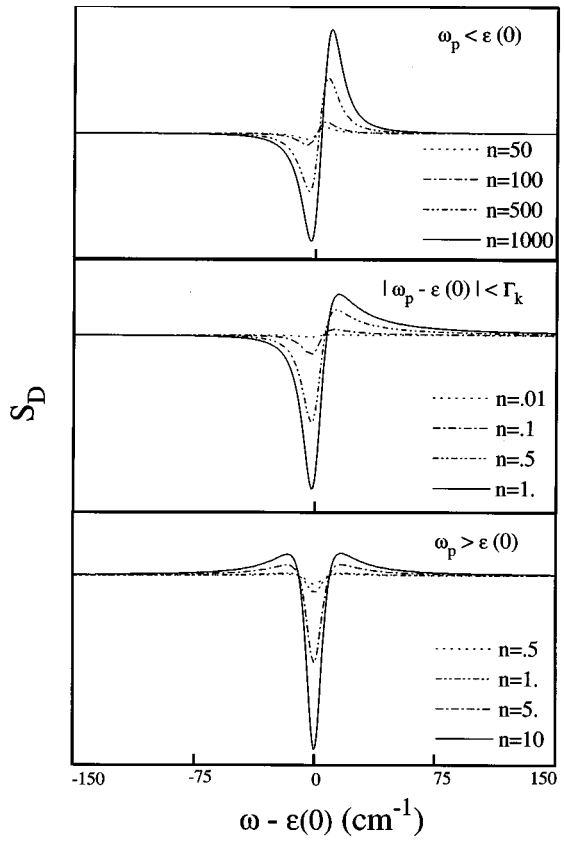

FIG. 3. Differential absorption for a periodic one-dimensional aggregate. For several pump intensities $I_p \propto |\mathscr{E}_p|^2$, $I_p = nI_0$, with $I_0 = 0.1$ MW/cm^2. Upper panel: for ω_p tuned below the bandedge, $\omega_p - \epsilon(0) = -625$ cm^{-1}. Middle panel: for ω_p close to the bandedge, $\omega_p - \epsilon(0) = -5$ cm^{-1}. Bottom panel: for ω_p inside the band, $\omega_p - \epsilon(0) = 625$ cm^{-1}.

The linear pulse absorption (in the absence of the pump) is given by

$$S_0(\omega) = \mathrm{Im}\ R(\omega, \omega_p, [\mathscr{E}_p = 0]) = \mu^2\ \mathrm{Im}[G(\omega, \mathbf{k}=0) + G^*(-\omega, \mathbf{k}=0)] \tag{3.8}$$

and the differential probe absorption is given by

$$S_D(\omega; \omega_p, [\mathscr{E}_p]) \equiv \mathrm{Im}\ \mathscr{R}(\omega; \omega_p, [\mathscr{E}_p]) - \mathrm{Im}\ \mathscr{R}(\omega; \omega_p, [\mathscr{E}_p = 0]), \tag{3.9}$$

where

$$\mathscr{R}(\omega; \omega_p, [\mathscr{E}_p]) \equiv \mathscr{R}(\omega, \mathbf{k}=0; \omega_p, \mathbf{k}_p = 0, [\mathscr{E}_p]). \tag{3.10}$$

We now apply these results to an infinite one-dimensional periodic aggregate with nearest neighbor interaction,

$$\epsilon(\mathbf{k}) = \Omega - 2J\ \cos(\mathbf{k}a), \tag{3.11}$$

where $J>0$ is a transfer matrix element, the band edge energy is $\epsilon(0) = \Omega - 2J$, and a is the lattice constant. In all calculations we used the parameters $J = 312.5$ cm^{-1}, and $\mu = 0.5$ Debye,[40] which are typical for anthracene. We further assumed a wave-vector-independent width $\eta(\mathbf{k}) = \eta = 10$ cm^{-1}.

The solid curve in Fig. 2(a) shows the linear absorption lineshape S_0. The differential absorption S_D for various pump intensities is displayed in Fig. 3. These results can be interpreted by noting that the Stark self-energy is proportional to

$$\Sigma^{(s)}(\omega; \omega_p, [\mathscr{E}_p]) \propto \overline{\Gamma}(\omega + \omega_p, \mathbf{k} + \mathbf{k}_p = 0), \tag{3.12}$$

and $\omega \approx \epsilon(0)$. When ω_p is tuned below the band (upper panel), $\Sigma^{(s)}$ is real, and the differential absorption assumes a dispersive form, reflecting a blue shift of the total absorption $(S_0 + S_D)$. When ω_p is tuned inside the band (bottom panel), $\Sigma^{(s)}$ is essentially purely imaginary and contributes a dynamical line broadening to the Lorentzian profile of the differential absorption. When ω_p is close to the bandedge (middle panel), the real and imaginary parts of $\Sigma^{(s)}$ are comparable and the differential absorption has an asymmetric profile.

IV. SIGNATURES OF STATIC DIAGONAL DISORDER IN OPTICAL STARK SPECTROSCOPY

The structure of organic aggregates usually contains various types of disorder (e.g., intermolecular separations, relative orientations and impurities). These reflect the relatively weak intermolecular forces which makes fluctuations more likely compared with inorganic crystals. To explore the effects of disorder we incorporate static Gaussian diagonal disorder to the model of Sec. III. We assume that the energies Ω_n are given by $\Omega_n = \Omega + U_n$, where U_n are independent variables with a Gaussian distribution.

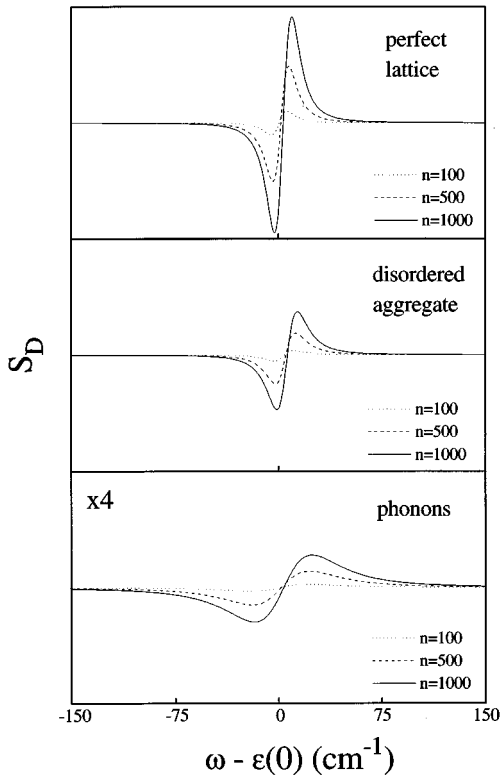

FIG. 4. Differential absorption for ω_p tuned below the bandedge ($\omega_p-\epsilon(0)=-625$ cm^{-1}) for a periodic one-dimensional aggregate and various pump intensities. Top panel: purely electronic system, no coupling with nuclear degrees of freedom. Middle panel: with diagonal disorder, $\sigma=10$ cm^{-1}. Bottom panel: with coupling to acoustic phonons $F_{\rm ac}=50$ cm^{-1}, $T=100$ K.

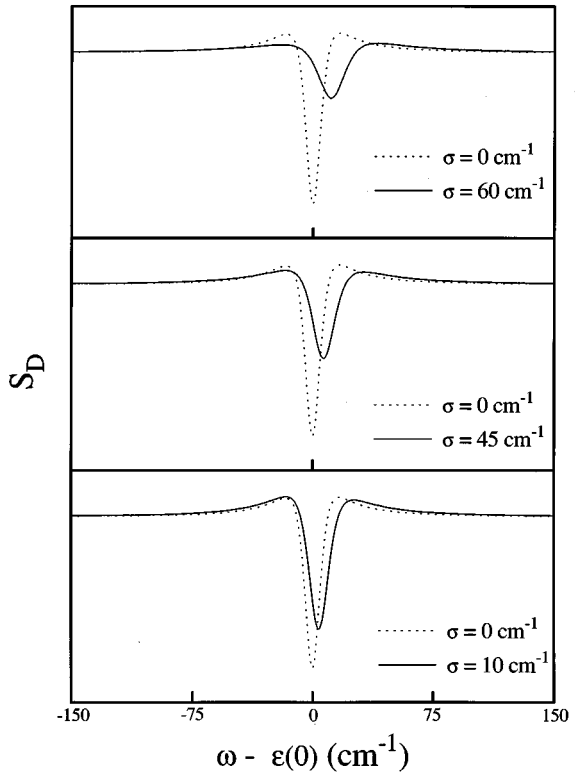

FIG. 5. Differential absorption for ω_p inside the band ($\omega_p-\epsilon(0)=625$ cm^{-1}) for an aggregate with different diagonal disorder parameter σ. Dashed line: no disorder, $\sigma=0$.

$$\langle U_n\rangle=0,\langle U_m U_n\rangle=\sigma^2\delta_{mn}, \tag{4.1}$$

and $\langle\cdots\rangle$ denotes averaging over static disorder. Cooperative radiative decay[41] and effects of exciton localization (i.e., Anderson localization) on the optical properties have been studied.[42–44] The necessary Green functions have been calculated in Ref. 4. The one-exciton Green function $G(\omega,\mathbf{k})$ is given by

$$G(\omega,\mathbf{k})=\frac{1}{\omega-\epsilon(\mathbf{k})-\Sigma(\omega)+i\eta(\mathbf{k})/2}, \tag{4.2}$$

where the self-energy representing the effects of disorder is calculated by solving the self-consistent equation:

$$\Sigma(\omega)=\sigma^2\int d\mathbf{k}\,\frac{1}{\omega-\epsilon(\mathbf{k})-\Sigma(\omega)+i\eta(\mathbf{k})/2}. \tag{4.3}$$

The two-exciton scattering matrix is

$$\overline{\Gamma^{(t)}}=\overline{\Gamma^{(a)}}+\overline{\Gamma^{(b)}} \tag{4.4}$$

with $\overline{\Gamma^{(a)}}$ given by Eq. (3.4), and

$$\overline{\Gamma^{(b)}}(-\omega-\mathbf{k};\omega_p\mathbf{k}_p,-\omega_p-\mathbf{k}_p,\omega\mathbf{k})$$
$$\equiv\frac{\sigma^2}{\Gamma_0}\int d\mathbf{p}\,2\pi\delta(\omega_p-\epsilon(\mathbf{p}))\overline{\Gamma}(\mathbf{k}+\mathbf{p},\omega+\omega_p). \tag{4.5}$$

The probe absorption is now given by Eqs. (3.9) with G and $\overline{\Gamma^{(t)}}$ given by Eqs. (4.2)–(4.5). In Fig. 2(a) we display the linear absorption for various values of the disorder parameter σ. The self-energy Σ is complex, and as σ increases, the line shape broadens and undergoes a blue shift. In Fig. 4 we display the differential absorption for ω_p tuned well below the bandedge for a disordered aggregate. For comparison we show in the top panel the same quantity in the absence of disorder $\sigma=0$. Both systems show a similar blue shift, since $\overline{\Gamma^{(b)}}$ vanishes in this case, $\overline{\Gamma^{(t)}}=\overline{\Gamma^{(a)}}$, and we can neglect the self-energies in $G(\omega_p)$, $G(\omega')$ and in $G(\omega+\omega_p-\omega')$ in Eq. (3.4). These results are in qualitative agreement both with the experimental work of Johnson *et al.*[33] on pump–probe spectra of BIC J aggregate and with numerical simulations performed using the sum over states expression for the nonlinear response.[34] In Fig. 5 we show the differential absorption for different values of disorder parameter σ when ω_p is tuned within the band (solid curves). For comparison we also give the signal in the absence of disorder (dashed curves). We see an additional blue shift induced by disorder. The reason is that $\overline{\Gamma^{(b)}}\propto\sigma^2/\Gamma_0$, and Re $\overline{\Gamma^{(t)}}$ which determines the blue shift is proportional to $\sigma^2|\mathscr{E}_p|^2$. In addition, $\Sigma(\omega)$ in (4.3) is complex and also contributes to the line shift. Figures 4 and 5 thus clearly show enhancement of both of the dynamical broadening and spectral shift due to disorder.

V. EFFECTS OF PHONONS

To incorporate the dynamical effects of phonon we adopt a model of harmonic phonons with exciton–phonon interac-

tion linear in phonon operators. The pump probe signal for a two electronic level model coupled with phonons with a Brownian oscillator spectral density can be calculated exactly for an arbitrary pump intensity.[45] In the case of molecular aggregates, $\hat{H}_{\rm mat}$ [Eq. (2.1)] can be written in the form:[6]

$$\hat{H}_{\rm mat}=\Omega\sum_m \hat{B}_m^+\hat{B}_m+\sum_{m\neq n} J_{mn}\hat{B}_m^+\hat{B}_n+\sum_{m,n}\Omega_{mn}\hat{b}_m^+\hat{b}_n + \sum_{mnl} V_{mnl}\hat{B}_m^+\hat{B}_n(\hat{b}_l^+ + \hat{b}_l). \tag{5.1}$$

The first three terms represent the free excitons and phonons energy, the last is the exciton–phonon interaction. The sum over m and n in the fourth term includes diagonal on-site coupling $n=m$ as well as off diagonal coupling. Optical phonons usually couple through the former terms and acoustic phonons through the latter.

In the momentum domain, this Hamiltonian assumes the form

$$\hat{H}_{\rm mat}=\int d\mathbf{q}\{\epsilon(\mathbf{q})\hat{B}_{\mathbf{q}}^+\hat{B}_{\mathbf{q}}+\Omega(\mathbf{q})\hat{b}_{\mathbf{q}}^+\hat{b}_{\mathbf{q}}\} + \int d\mathbf{p}\, d\mathbf{q}\{V(\mathbf{q},\mathbf{q}-\mathbf{p})\hat{B}_{\mathbf{p}}^+\hat{B}_{\mathbf{q}}\hat{b}_{\mathbf{q}-\mathbf{p}}^+ + V^*(\mathbf{q},\mathbf{q}-\mathbf{p})\hat{B}_{\mathbf{q}}^+\hat{B}_{\mathbf{p}}\hat{b}_{\mathbf{q}-\mathbf{p}}^+\}, \tag{5.2}$$

where $\epsilon(\mathbf{q})$ is the exciton energy [Eq. (3.11)] and

$$V(\mathbf{q},\mathbf{q}-\mathbf{p})\equiv\sum_{mnl} e^{i\mathbf{q}\cdot(\mathbf{R}_n-\mathbf{R}_l)-i\mathbf{p}\cdot(\mathbf{R}_m-\mathbf{R}_l)}V_{mnl}. \tag{5.3}$$

Neglecting the real part of the self-energy, the one-exciton Green function $G(\omega,\mathbf{k})$ becomes[4]

$$G(\omega,\mathbf{k})=\frac{1}{\omega-\epsilon(\mathbf{k})+i\Sigma(\mathbf{k})+i\,\eta(\mathbf{k})/2}, \tag{5.4}$$

where the phonon self-energy is given by

$$\Sigma(\mathbf{k})=\frac{1}{2}\int d\mathbf{p}\; f(\mathbf{p},\mathbf{k}), \tag{5.5}$$

with

$$f(\mathbf{p},\mathbf{p}')=2\pi|V(\mathbf{p}',\mathbf{p}'-\mathbf{p})|^2(1+N[\Omega(\mathbf{p}'-\mathbf{p})])\,\delta(\epsilon(\mathbf{p})-\epsilon(\mathbf{p}')-\Omega(\mathbf{p}'-\mathbf{p}))+2\pi|V(\mathbf{p},\mathbf{p}-\mathbf{p}')|^2\times N[\Omega(\mathbf{p}-\mathbf{p}')]\,\delta(\epsilon(\mathbf{p})-\epsilon(\mathbf{p}')-\Omega(\mathbf{p}-\mathbf{p}')). \tag{5.6}$$

$N_\Omega=[\exp(\Omega/kT)-1]^{-1}$ are the Bose occupation numbers and T is the temperature. The exciton-acoustic phonon coupling function is[6]

$$V(\mathbf{k},\mathbf{q})=F_{\rm ac}\,\frac{\cos[(\mathbf{k}+\mathbf{q}/2)a]\sin(\mathbf{q}a/2)}{\sqrt{\sin|\mathbf{q}a/2|}}, \tag{5.7}$$

and the phonon spectrum modeled as

$$\Omega_{\rm ac}(\mathbf{q})=\Omega_{\rm ac}\,\sin|\mathbf{q}a/2|. \tag{5.8}$$

The two-exciton scattering matrix is given by Eq. (4.4) with

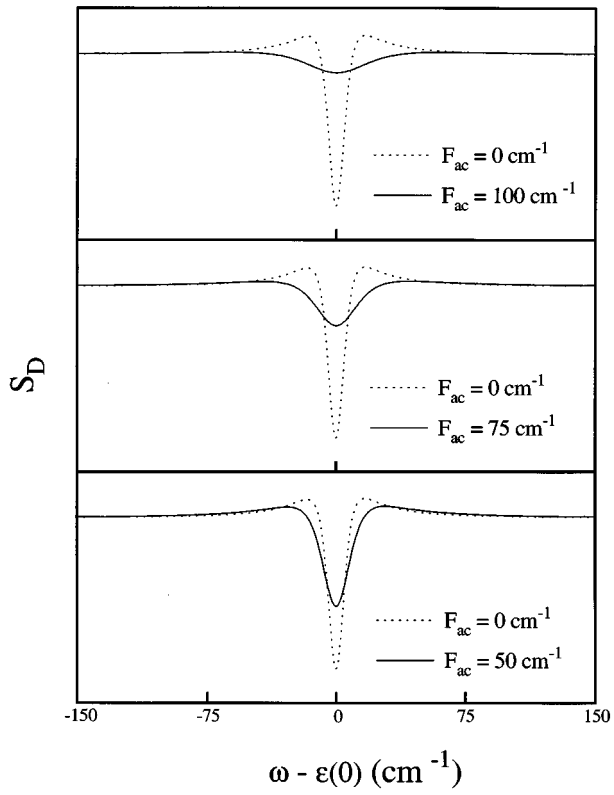

FIG. 6. Differential absorption for various exciton-phonon coupling strength $F_{\rm ac}$. Dashed line: no exciton–phonon coupling.

$$\overline{\Gamma}^{(b)}(-\omega-\mathbf{k};\omega_p\mathbf{k};\omega_p\mathbf{k}_p,-\omega_p-\mathbf{k}_p,\omega\mathbf{k}) \equiv\frac{C}{\Gamma_0}\int d\mathbf{p}'\; g(\mathbf{p}',\mathbf{k},\omega_p)\int d\mathbf{p}\; e^{-\epsilon\mathbf{k}/kT} \times\overline{\Gamma}^{(a)}(\mathbf{k}+\mathbf{p},\epsilon(\mathbf{p})-\omega), \tag{5.9}$$

where we have used the following notation:

$$\Gamma_0\equiv C\int d\mathbf{p}\;\Gamma(\mathbf{p})\exp\left(-\frac{\epsilon(\mathbf{p})}{kT}\right),$$

$$g(\mathbf{p},\mathbf{q}_0;\Omega)=2\pi|V(\mathbf{q}_0,\mathbf{q}_0-\mathbf{p})^2(1+N[\Omega(\mathbf{q}_0-\mathbf{p})]) \times\delta(\Omega-\epsilon(\mathbf{p})-\Omega(\mathbf{q}_0-\mathbf{p}))+2\pi|V(\mathbf{p},\mathbf{p}-\mathbf{q}_0)|^2 \times N[\Omega(\mathbf{p}-\mathbf{q}_0)]\delta(\Omega-\epsilon(\mathbf{p})-\Omega(\mathbf{p}-\mathbf{q}_0)), \tag{5.10}$$

$$C\equiv\left\{\int d\mathbf{p}\;\exp\left(-\frac{\epsilon(\mathbf{p})}{kT}\right)\right\}^{-1}.$$

We note that both $\Sigma(\mathbf{k})$ and $\overline{\Gamma}^{(b)}$ are quadratic in the coupling V. In the following calculations we assumed $\Omega_{\rm ac}=67$ cm^{-1} (Ref. 40) and $T=100$ K, and varied the coupling strength $F_{\rm ac}$. The linear absorption is displayed in Fig. 2(b). The phonon self-energy [Eq. (5.5)] is purely imaginary, and the lineshapes broaden as $F_{\rm ac}$ is increased. The differential absorption when ω_p is tuned off resonant is displayed in the bottom panel in Fig. 4. Since $\overline{\Gamma}^{(b)}=0$, this case looks qualitatively similar to the pure and disordered aggregates

(other two panels). Calculations for ω_p tuned inside the band are displayed in Fig. 6. Since the exciton self-energy $\Sigma(\mathbf{k})$ in Eq. (5.5) is purely imaginary, the differential absorption broadens (but does not shift) as $F_{\rm ac}$ is increased. This is different from the case of disorder (Fig. 5) which shows shift as well.

VI. DISCUSSION

In the article we applied the Keldysh correlation function formulation of nonlinear response to optical Stark spectroscopy of Frenkel excitons including static diagonal disorder or coupling with phonons. The differential absorption lineshape to lowest order in pump intensity can be expressed in terms of the one exciton Green function and the two-exciton scattering matrix which determine the third-order response. This suggests that to lowest order in the pump intensity the Stark self-energy $\Sigma^{(s)}$ can be expressed in terms of the response functions $R^{(1)}$ and $R^{(3)}$. We shall now derive a more general relation between the Stark self-energy and the response functions $R^{(n)}$, which holds to all orders in the pump field. The response functions $R^{(n)}$ are defined through the expansion:[4]

$$P(\mathbf{r},t)=\sum_{n=0}^{\infty}\frac{1}{n!}\int d\mathbf{r}_1\,dt_1\ldots\int d\mathbf{r}_n\,dt_n \times R^{(n)}(\mathbf{r}t;\mathbf{r}_1t_1,\ldots,\mathbf{r}_nt_n)\mathscr{E}(\mathbf{r}_1,t_1)\ldots\mathscr{E}(\mathbf{r}_n,t_n) \tag{6.1}$$

with

$$R^{(n)}(\mathbf{r}t;\mathbf{r}_1t_1,\ldots,\mathbf{r}_nt_n) = i^n\langle\hat{P}_+(\mathbf{r},t)\hat{P}_-(\mathbf{r}_1,t_1)\ldots\hat{P}_-(\mathbf{r}_n,t_n)\rangle. \tag{6.2}$$

In $(\mathbf{k},\omega)$ space we have

$$R^{(3)}(-\omega-\mathbf{k};\omega_1\mathbf{k}_1,-\omega_2-\mathbf{k}_2,\omega_3\mathbf{k}_3) = \int\int\int dx_1\,dx_2\,dx_3\,R^{(3)}(\mathbf{r}t;\mathbf{r}_1t_1,\mathbf{r}_2t_2,\mathbf{r}_3t_3) \times e^{i\omega_1(t-t_1)-i\mathbf{k}_1\cdot(\mathbf{r}-\mathbf{r}_1)}e^{-i\omega_2(t-t_2)+i\mathbf{k}_2\cdot(\mathbf{r}-\mathbf{r}_2)} \times e^{i\omega_3(t-t_3)-i\mathbf{k}_3\cdot(\mathbf{r}-\mathbf{r}_3)}, \tag{6.3}$$

where $x_i=(t_i,\mathbf{r}_i)$. The response function $\mathscr{R}$ [Eq. (2.9)] in the presence of the pump can be written in the form

$$\mathscr{R}(\omega\mathbf{k};\omega_p\mathbf{k}_p,[\mathscr{E}_p])=\frac{R^{(1)}(\omega\mathbf{k})}{1+A(\omega\mathbf{k};\omega_p\mathbf{k}_p,[\mathscr{E}_p])}, \tag{6.4}$$

with

$$A(\omega\mathbf{k};\omega_p\mathbf{k}_p,[\mathscr{E}_p])=\sum_{n=1}^{\infty}A^{(2n)}(\omega\mathbf{k};\omega_p\mathbf{k}_p)|\mathscr{E}_p|^{2n}. \tag{6.5}$$

Substituting the electric field [Eq. (2.8)] in Eq. (6.1), expanding to linear order in $\mathscr{E}_s$, and comparing the expansion of $\mathscr{R}$ in powers of $\mathscr{E}_p$ order by order with the expansion (6.4) gives

$$A^{(2)}(\omega\mathbf{k};\omega_p\mathbf{k}_p)=-R^{(3)}(-\omega-\mathbf{k};\omega_p\mathbf{k}_p,-\omega_p-\mathbf{k}_p,\omega\mathbf{k}) \times\{R^{(1)}(\omega\mathbf{k})\}^{-1},$$

$$A^{(4)}(\omega\mathbf{k};\omega_p\mathbf{k}_p) = R^{(5)}(-\omega-\mathbf{k};\omega_p\mathbf{k}_p,-\omega_p-\mathbf{k}_p,\omega_p\mathbf{k}_p,-\omega_p-\mathbf{k}_p,\omega\mathbf{k}) \times\{R^{(1)}(\omega\mathbf{k})\}^{-1} +\{R^{(3)}(-\omega-\mathbf{k};\omega_p\mathbf{k}_p,-\omega-\mathbf{k}_p,\omega\mathbf{k})\}^2 \times\{R^{(1)}(\omega\mathbf{k})\}^{-2}. \tag{6.6}$$

Equations (6.6) provide a general connection between the Stark self-energy and the nonlinear optical response functions $R^{(n)}$. Similar expressions can be derived for the higher-order terms. A relation between the Stark shift and the derivative of the linear response function $R^{(1)}(\omega)$ with respect to ω has been proposed in Ref. 31 for a two-level model. This is in good agreement with Eq. (6.6) since for a two-level molecule $R^{(3)}(-\omega;\omega_p,-\omega_p,\omega)$ can be expressed in terms of $dR^{(1)}(\omega_p)/d\omega_p$. Equation (6.6) show however that in general the Stark self-energy depends on higher-order response functions and may not be simply related to $R^{(1)}$. It is possible to calculate optical response functions using expressions based on sum over states.[20] These show large cancellations of terms in calculating the Stark effect. Such cancellations for $R^{(3)}$ in molecular aggregates have been demonstrated in Ref. 5. The Green function technique used here expresses the Stark self-energy in terms of the exciton–exciton scattering matrix which is a measure the anharmonicity of the Frenkel exciton system. It does not suffer from such cancellations. It also provides a physical picture of exciton dynamics in terms of weakly coupled slightly anharmonic oscillators.

Our results suggest that optical Stark spectroscopy can be used to probe the frequency and wave-vector-dependent two-exciton scattering matrix $\Gamma(\omega,\mathbf{k})$. We have shown both analytically and numerically that if the pump is tuned below the exciton band, the differential absorption is very similar in all three cases considered (purely electronic aggregate, disordered, and with exciton–phonon coupling), and that the Stark spectrum is related to $\Gamma(\omega+\omega_p,\mathbf{k}\approx0)$. This similarity is maintained when ω_p is near the bandedge. The picture is more interesting when the pump field is tuned inside the exciton band. In the purely electronic model we still probe $\Gamma(\omega+\omega_p,\mathbf{k}\approx0)$. In disordered aggregates we have an enhancement of the Stark effect given by the ratio of the dephasing rate related to the static disorder to the inverse lifetime (which is typical for the degenerate four-wave mixing spectroscopy). Another characteristic feature of the disordered system is that the signal is given by $\Gamma(\omega+\omega_p,\mathbf{k}')$ with $\epsilon(\mathbf{k}')=\omega_p$. This means that real excitations are created by the pump field, and their energy is not affected by the excitation process since the scattering induced by static disorder is elastic. Coupling with phonons yields a similar enhancement with the only difference from the disorder case is that the dephasing rate is related to the exciton–phonon scattering. However the signal is in this case related to

$\overline{\Gamma}(\omega+\omega',\mathbf{k}')$ with $\omega'=\epsilon(\mathbf{k}')$ and $\omega'-\epsilon(0)\sim kT$. This reflects the inelastic nature of exciton–phonon scattering; the distribution of real excitons with energy ω_p created by the pump field is equilibrated thermally and assumes the Boltzmann form at long times.

ACKNOWLEDGMENTS

The support of the National Science Foundation, the Air Force Office of Scientific Research, and the NSF Center for Photoinduced Charge Transfer is gratefully acknowledged.

[1] V. L. Broude, E. I. Rashba, and E. F. Sheka, *Spectroscopy of Molecular Excitons* (Springer-Verlag, Berlin, 1985).
[2] D. Möbius and H. Kuhn, J. Appl. Phys. **64**, 5138 (1988); D. Möbius and H. Kuhn, Isr. J. Chem. **18**, 375 (1979).
[3] Special Issue, Physica Status Solidi **189** (1995).
[4] V. Chernyak, N. Wang, and S. Mukamel, Phys. Rep. **263**, 213 (1995).
[5] S. Mukamel, in *Molecular Nonlinear Optics*, edited by J. Zyss (Academic, New York, 1994) Vol. 1; F. C. Spano and S. Mukamel, Phys. Rev. A **40**, 5783 (1989); F. C. Spano and S. Mukamel, Phys. Rev. Lett. **66**, 1197 (1991).
[6] A. S. Davydov, *Theory of Molecular Excitons* (Plenum, New York, 1971); M. Pope and C. E. Swenberg, *Electronic Processes in Organic Crystals* (Oxford, New York, 1982); J. Singh, *Excitation Energy Transfer Processes in Condensed Matter* (Plenum, New York, 1994).
[7] J. Knoester and S. Mukamel, Phys. Rep. **205**, 1 (1991).
[8] H. Haug and S. W. Koch, *Quantum Theory of the Optical and Electronic Properties of Semiconductors* (World Scientific, Singapore, 1993).
[9] M. L. Steigerwald and L. E. Brus, Acc. Chem. Res. **23**, 183 (1990); M. Bawendi, M. L. Steigerwald and L. E. Brus, Annu. Rev. Phys. Chem. **44**, 281 (1990).
[10] A. H. Hertz, Adv. Colloid Interface Sci. **8**, 237 (1977).
[11] A. A. Muenter *et al.*, J. Phys. Chem. **96**, 2783 (1992).
[12] F. C. Spano, J. R. Kuklinski, and S. Mukamel, J. Chem. Phys. **94**, 7534 (1991); F. C. Spano, J. R. Kuklinski, and S. Mukamel, Phys. Rev. Lett. **65**, 211 (1990); J. Grad, G. Hernandez, and S. Mukamel, Phys. Rev. A **37**, 3835 (1988).
[13] H. Fidder, J. Knoester, and D. A. Wiersma, Chem. Phys. Lett. **171**, 529 (1990).
[14] E. I. Haskal, Y. Zhang, P. E. Burrows, and S. R. Forest, Chem. Phys. Lett. **219**, 325 (1994); F. F. So, S. R. Forrst, Y. Q. Shi, and W. H. Steier, Appl. Phys. Lett. **56**, 674 (1990); F. F. So and S. R. Forrest, Phys. Rev. Lett. **62**, 2649 (1991).
[15] R. van Grondelle, J. P. Dekker, T. Gillbro, and V. Sundstrom, Biochim. Biophys. Acta **1187**, 1 (1994); G. McDermont *et al.*, Nature **374**, 517 (1995); W. Kuhlbrandt, D. N. Wang, and Y. Fujiyoshi, *ibid.* **367**, 614 (1994).
[16] N. R. S. Reddy, H. van Amerongen, S. L. S. Kwa, R. van Grondelle, and G. J. Small, J. Phys. Chem. **98**, 4729 (1994).
[17] M. Du, X. Xie, L. Mets, and G. R. Fleming, J. Phys. Chem. **98**, 4736 (1994).
[18] T. Bittner, G. P. Wiederrecht, K. D. Irrgang, G. Renger, and M. R. Wasielewski, Chem. Phys. **194**, 311 (1995).
[19] S. Mukamel, *Principles of Nonlinear Optical Spectroscopy* (Oxford, New York, 1995).
[20] B. E. Kohler and J. C. Woehl, *Measuring Internal Electric Fields with Atomic Resolution* (private communication); B. E. Kohler, R. I. Personov, and J. C. Woehl, in *Laser Techniques in Chemistry,* Series Techniques in Chemistry (Wiley, New York, 1995), Vol. 23; D. S. Gottfried, J. W. Stocker, and S. G. Boxer, Biochim. Biophys. Acta **1059**, 63 (1991).
[21] H. Fidder, J. Knoester, and D. A. Wiersma, J. Chem. Phys. **98**, 6564 (1993).
[22] R. M. Hochstrasser and J. D. Whiteman, J. Chem. Phys. **56**, 9564 (1972).
[23] K. Minoshita, M. Taiji, K. Misawa, and T. Kobayashi, Chem. Phys. Lett. **218**, 67 (1994).
[24] A. Mysyrowicz, D. Hulin, A. Antonetty, A. Migus, W. T. Masselink, and H. Mordoc, Phys. Rev. Lett. **56**, 2748 (1986).
[25] S. D. Halle, M. Yoshizawa, H. Matsuda, S. Okada, H. Nakanishi, and T. Kobayashi, J. Opt. Soc. Am. B **11**, 731 (1994).
[26] G. J. Blanchard, J. P. Heritage, A. C. von Lehmen, M. K. Kelly, G. L. Baker, and S. Eteman, Phys. Rev. Lett. **63**, 887 (1989).
[27] J. R. G. Thorne, S. T. Repinec, S. A. Abrash, J. M. Ziegler, and R. M. Hochstrasser, Chem. Phys. **146**, 315 (1990); G. J. Blanchard *et al.*, Phys. Rev. Lett. **63**, 887 (1989).
[28] S. Schmitt-Rink and D. S. Chemla, Phys. Rev. Lett. **57**, 2752 (1986); S. Schmitt-Rink, D. S. Chemla, and H. Haug, Phys. Rev. B **37**, 941 (1988).
[29] M. Combescot and R. Combescot, Phys. Rev. Lett. **61**, 117 (1988).
[30] R. Zimmermann, Festkörperprobleme **30** (1990).
[31] M. Joffre, D. Hulin, A. Migus, and A. Antonetti, J. Mod. Opt. **35**, 1951 (1988).
[32] D. S. Chemla, D. A. B. Miller, and S. Schmitt-Rink, Phys. Rev. Lett. **59**, 1018 (1987).
[33] A. Johnson, S. Kumazaki, and K. Yoshihara, Chem. Phys. Lett. **211**, 511 (1993).
[34] F. Spano, Chem. Phys. Lett. **220**, 365 (1991).
[35] F. F. So and S. R. Forrest, Phys. Rev. Lett. **56**, 2649 (1991).
[36] D. P. Craig and T. Thirunamachandran, *Molecular Quantum Electrodynamics* (Academic, London, 1984).
[37] J. A. Leegwater and S. Mukamel, Phys. Rev. A **46**, 452 (1992); N. Wang, J. A. Leegwater, and S. Mukamel, J. Chem. Phys. **98**, 5899 (1993).
[38] L. V. Keldysh, Soviet Phys. JETP **20**, 1018 (1965); E. M. Lifshitz and L. P. Pitayevsky, *Physical Kinetics* (Pergamon, Oxford, 1981).
[39] A. A. Abrikosov, L. P. Gorkov, and I. Ye. Dzyaloshinsky, *Quantum Field Theoretical Methods in Statistical Physics* (Pergamon, Oxford, 1965).
[40] G. S. Morris and M. G. Sceats, Chem. Phys. **3**, 342 (1974).
[41] F. C. Spano and S. Mukamel, J. Chem. Phys. **91**, 683 (1989).
[42] R. F. Loring and S. Mukamel, J. Chem. Phys. **85**, 1738 (1986).
[43] H. P. Trommsdorf and R. M. Hochstrasser, J. Lumin. **53**, 170 (1992); A. Tilgner, H. P. Trommsdorf, J. M. Zeigler, and R. M. Hochstrasser, J. Chem. Phys. **96**, 781 (1992).
[44] J. Knoester, J. Chem. Phys. **99**, 8466 (1993).
[45] Y. Tanimura and S. Mukamel, J. Phys. Soc. Jpn. **63**, 66 (1994).